

# Effect of Molecular Weight Distribution of Poly(oxytetramethylene)glycol on Cut Growth Resistance of Polyurethane

YOSHIO KANEKO,\* YOJI WATABE,\* TAKESHI OKAMOTO,\*  
YUTAKA ISEDA,\*\* and TSUTOMU MATSUNAGA,\* *Bridgestone Tire Co.  
Ltd., 2800-1 Ogawahigashi, Kodaira, Tokyo 187, Japan*

## Synopsis

A new method is proposed to improve the cut growth resistance of polyether-based polyurethane elastomers, i.e., polyethers used in this method are characterized by a double-humped distribution of molecular weight (DHDM), prepared by blending low-molecular-weight components and high-molecular-weight ones. The measurements of stress-strain curves, viscoelastic properties, and DSC thermograms of polyurethane elastomers before and after fatigue tests indicate that the destruction of the super molecular structure because of fatigue is smaller in the elastomer by our method, while in the conventional elastomer it is greatly destructed to change into fibrous structure. Further, the broad line NMR measurements show that the molecular motion of DHDM-type elastomers is more active, which is considered to contribute to the improved cut growth resistance of the elastomers.

## INTRODUCTION

For practical importance, few articles dealing with flex crack resistance of polyurethane elastomers have been published. Several ways have been known to improve the flex crack resistance of polyurethane elastomers:

(1) decreasing modulus by reducing the content of hard segments or compounding plasticizers;

(2) decreasing chemical crosslink density by adjusting the molar ratio of active hydrogens to isocyanate groups to a value larger than 1.0 (ref. 1); and

(3) decreasing the molecular weight of the polyurethane elastomer.<sup>2</sup>

McGillvary combined (1) and (2) to achieve so excellent a flex crack resistance as to be durable for tire testings.<sup>3</sup> However, for tire application, not only crack initiation but also cut growth resistance is important. In this case, tear resistance might be considered to be one of the most important factors as well. Several attempts<sup>4-7</sup> have been made to increase the tear resistance of segmental block polyurethane elastomers:

(4) using chain extenders and diisocyanate compounds of bulky and symmetrical molecular structure, as shown by Buist and Gudgeon<sup>4</sup>;

(5) employing a polymer glycol that is polar and that easily crystallizes by elongation, for instance, poly(ethylene adipate)glycol<sup>5</sup>;

(6) increasing the length of hard segments by keeping their fraction constant<sup>6</sup>; and

(7) modifying the polyurethane by the interpenetrating polymer network (IPN) method.<sup>7</sup>

\* New Products Development Division.

\*\* Tire Designing Department.

In this article we would like to disclose that segmental polyurethane elastomers prepared from specially designed polyethers with double-humped distribution of molecular weight (DHDM) should be improved in cut growth resistance without any significant disadvantage to other mechanical properties of conventional polyurethane elastomers. This conclusion is derived through discussion of cut growth resistance, tensile properties, viscoelastic properties, heat of fusion, and half-width of broad line NMR comparing DHDM types of polyurethanes with conventional ones.

## EXPERIMENTAL

### Materials

All the poly(oxytetramethylene)glycols (PTMGs) employed were from Dainihon Ink Co., Ltd.; their molecular weights are listed in Table II. PTMG6000, PTMG10000, and PTMG20000 were prepared from PTMG780 and PTMG2080, as follows, to prevent the resulting elastomers from crystallization at low temperatures: A mixture of 30 g of PTMG780 and 70 g of PTMG2080 was dehydrated at 80°C and 4 torr for 1 hr, followed by the addition of a calculated amount of hexamethylene diisocyanate (HMDI) from eq. (1) and heating at 80°C for 16 hr:

$$P = (-M_1 + M_2)/(I + M_2) \quad (1)$$

were  $M_1$  is the number-average molecular weight of the PTMG mixture at the initial stage,  $M_2$  is the same after a chain extension reaction,  $I$  is the molecular weight of HMDI, and  $P$  represents the mole numbers of HMDI per 1 mole the PTMG mixture. According to eq. (1),  $P$  is 0.748, 0.847, and 0.923 in response to the required  $M_2$  of 6000, 10,000, and 20,000, respectively, because  $M_1$  is 1390 and  $I$  is 168.

Table I shows the heats of fusion ( $\Delta H_f$ ) and melting temperatures ( $T_m$ ) for various raw PTMGs. The values of  $\Delta H_f$  for PTMG6000 and PTMG20000 are much smaller than those for the other PTMGs, indicating their restricted crystallization.

Isocyanate-terminated PTMGs (prepolymers) were prepared as follows: One mole of the PTMG mixture, well dried in the same way as described above, was reacted with 2.01 mole of 2,4-tolylene diisocyanate (TDI) at 80°C for 8 hr. In

TABLE I  
Heats of Fusion and Melting Points for Crystalline Raw PTMG<sup>a</sup>

Molecular weight of PTMG	$H_f$ (cal/g)	$T_m$ (°C)
780	22	28, 31
1070	21	31
1580	20	32
2080	23	35
6000	10	28
20,000	8	28

<sup>a</sup> Prepared by extending a mixture of PTMG780 and PTMG2080 with hexamethylene diisocyanate.

order to determine the content of isocyanate groups [NCO content (wt %)], 1 g of the prepolymer was dissolved in 20 ml of 0.1*N* solution of di-*n*-butylamine in tetrahydrofuran (THF) at room temperature, and after 30 min the solution was titrated with 0.1*N* hydrochloric acid using bromocresol green as an indicator.

3,3'-Dichloro-4,4'-diaminodiphenylmethane (MOCA) was employed as a chain extender. The molar ratio of amino groups of MOCA to isocyanate groups of the prepolymer  $\text{NH}_2/\text{NCO}$  was 1.0 in all the test pieces. The mixtures of the prepolymer and MOCA were cured for 180 min at 100°C and then aged for a week at 30°C under a 50% humidity atmosphere.

### Measurements

Tensile strength at break [ $T_B$  (kg/cm<sup>2</sup>)] and elongation at break [ $E_B$  (%)] were measured at 25°C with 50 mm/min extension speed, using test pieces cut from 2-mm thick slab sheets with a ring dumbbell. Tear energy [ $\Gamma$  (kg/cm)] was measured according to the method proposed by Ninomiya<sup>8</sup> and Nishi,<sup>9</sup> using test samples (80 × 10 × 2 mm) having a 2-mm long cut at its margin perpendicular to the tensile direction.

The cut growth resistance under constant strain was tested by a De Mattia fatigue tester using test samples (100 × 10 × 1 mm) with a 2-mm wide cut at their centers perpendicular to the tensile direction. The maximum constant strain selected from 5 to 30% was applied to the samples repeatedly at 300 cycles/min with a distance of 50 mm between the two clamps. The number of cycles to break ( $N$ ) was counted. The cut growth resistance under constant stress was tested by means of an Instron Universal Tester using test samples (100 × 5 × 1 mm) with a 1-mm wide cut at their margins perpendicular to the tensile direction. The maximum constant stress selected from 45 to 62 kg/cm<sup>2</sup> was applied to the samples repeatedly at the crosshead speed of 200 mm/min with a distance of 50 mm between the two clamps. The number of cycles to break ( $N$ ) was counted.

Molecular weight distribution was measured by Waters Associates model 200. The columns consisted of Styragel 10<sup>6</sup>, 10<sup>5</sup>, 10<sup>4</sup>, and 10<sup>3</sup> Å. The eluent was THF at a flow rate of 1 ml/min at 35°C. Storage moduli [ $E'$  (kg/cm<sup>2</sup>)] and loss tangents ( $\tan \delta$ ) were measured by a dynamic mechanical spectrometer manufactured by Iwamoto Seisakusho Co., Ltd. at 100 Hz from -100 to 200°C. The heats of fusion for PTMGs [ $\Delta H_f$  (cal/g)] and the heats of fusion for crystalline hard segments were measured by a differential scanning calorimeter (DSC) by Perkin Elmer Co., Ltd. at 5°C/min scan rate. The half-width of broad line NMR spectrum [ $\Delta H^{1/2}$  (m G)] as a measure of degree of molecular motion was measured by a NMR spectrometer, which was an improved type of MH-60 by Nihon Denshi Co., Ltd.

## RESULTS AND DISCUSSION

### Critical Molecular Weight

In this article polyurethane elastomers prepared by our method are referred to as DHDM, since PTMGs used are characterized by double-humped distribution of molecular weight. On the other hand, conventional ones are referred as MDDM (mono dispersive distribution of molecular weight).

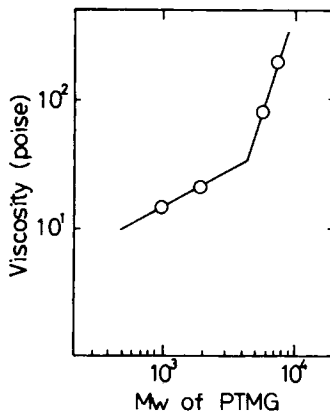


Fig. 1. Relationship between viscosity and number-average molecular weight of PTMG. Viscosity was measured by means of an Instron capillary rheometer at a shear rate of  $10^3 \text{ sec}^{-1}$  and at  $80^\circ\text{C}$ .

DHDM was prepared from a mixture of two PTMGs having big differences in molecular weight. The role of the higher-molecular-weight component is to give more elasticity to the elastomer. Though raw PTMG shows very active molecular motion, it loses this activity substantially after it is incorporated into the matrix of the elastomer. This is due to the effect of very strong pseudo-crosslinks by hard segments consisting of urea and urethane groups. The component should, therefore, have a molecular weight high enough to be free from the restriction by hard segments. The rheological critical molecular weight ( $M_c$ ), where intermolecular entanglements start to take place can be a measure of the molecular weight, described above.

Figure 1, which is privately communicated by Tsukamoto,<sup>10</sup> shows a relationship between viscosity and molecular weight of PTMGs. The  $M_c$  of PTMG is 4500, as seen from the inflection point in Figure 1.

### Tensile Properties

The recipes for all the samples are listed in Table II. In order to get elastomers with a wide hardness range, the NCO contents are varied from 1.38 to 6.75%. The contents of isocyanate groups for DHDM are adjusted to be similar to the values for MDDM by changing the molecular weight of the PTMGs and their blend ratio. Figure 2 shows a gel permeation chromatogram for a PTMG mixture used

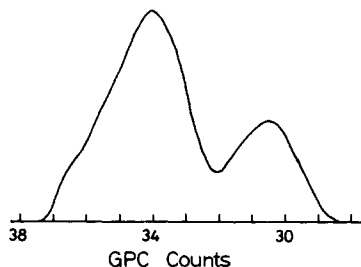


Fig. 2. GPC curve for D-7.

TABLE II  
 PTMGs and Prepolymers Used in the Experiments

No.	Molecular weight of PTMG		Blend ratio by weight		NCO content of prepolymer (wt %)
	(1)	(2)	(1)	(2)	
MDDM					
M1	6000		100	0	1.38
M2	3030		100	0	2.50
M3	2000	2900	35	65	2.95
M4	2480		100	0	2.96
M5	2240		100	0	3.69
M6	2080		100	0	4.05
M7	1580		100	0	4.39
M8	1580	1070	60	40	5.10
M9	1070		100	0	5.93
M10	880		100	0	6.75
DHDM					
D1	1070	20,000	43	57	2.60
D2	1580	20,000	61	39	2.90
D3	1070	20,000	56	44	3.45
D4	1070	6000	64	36	4.52
D5	780	6000	52	48	4.83
D6	1070	10,000	80	20	4.99
D7	780	20,000	68	32	5.25

in making the sample D-7, which shows two peaks at molecular weights of 800 and 20,000.

Figure 3 shows a relationship between  $M_{10}$  and NCO content. The 10% moduli for both MDDM and DHDM increase with increasing NCO content. It should be noticed particularly that they are plotted on the same curve. It indicates that high-molecular-weight component does not affect the ordering of hard segments. Similar result is obtained from a relationship between  $T_B$  and NCO content (Fig. 4). Tensile strength at break decreases substantially at 100°C. It is probably due to the softening of crystalline hard segments and incapability of stress-induced crystallization of soft segments at 100°C.

One of the differences in mechanical properties between the two elastomer systems can be seen in  $E_B$  (Fig. 5). Elongation at break for DHDM is about 100% larger than  $E_B$  for MDDM at any NCO content. The dependence of  $E_B$  on NCO

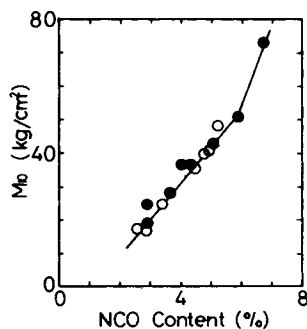


Fig. 3. Relationship between  $M_{10}$  and NCO content. (○) DHDM; (●) MDDM.

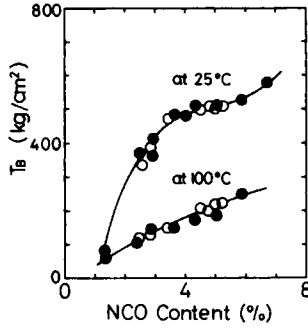


Fig 4. Relationship between tensile strength at break ( $T_B$ ) and NCO content. (○) DHDM; (●) MDDM.

content is apparently contrary to those of  $T_B$  and  $M_{10}$ , which can be explained by the decrease of the content of extensible soft segments with the increase of the NCO content.

**Cut Growth Resistance (1)**

The number of cycles to break ( $N$ ) by a De Mattia fatigue tester is plotted against  $M_{10}$  in Figure 6. The maximum strain was 25%. The comparison be-

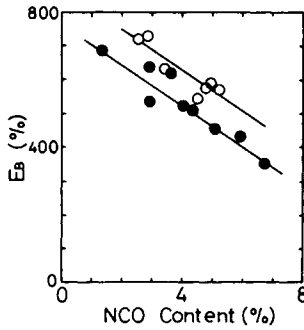


Fig. 5. Relationship between elongation at break ( $E_B$ ) and NCO content. (○) DHDM; (●) MDDM.

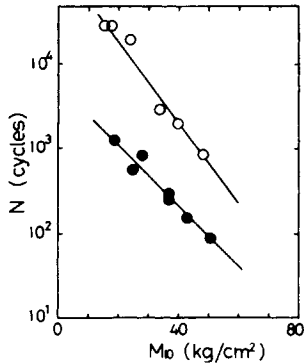


Fig. 6. Relationship between  $M_{10}$  and number of cycles to break ( $N$ ) under 25% constant strain. (○) DHDM; (●) MDDM.

tween the two elastomer systems should be done at the same  $M_{10}$ , since an elastomer of a lower modulus naturally shows better fatigue resistance under the constant repeated strain. As shown in Figure 6,  $N$  for DHDM is about one order of magnitude larger than that for MDDM at any  $M_{10}$ . Thus, incorporating a high-molecular-weight component to the polyurethane matrix is a new way to improve the cut growth resistance of the elastomer.

### Cut Growth Resistance (2)

In order to study the cut growth resistance in more detail, three test samples in Table III having almost the same value of  $M_{10}$  were subjected to the De Mattia fatigue test. Sample C for comparison with McGillvary's recipe helps us to discuss the good cut growth resistance for DHDM. The reported good flex crack resistance for sample C is apparently based on the combination of the following reasons: the increasing of  $\text{NH}_2/\text{NCO}$  ratio to 1.07 and incorporating of dioctylphthlate (DOP) as a plasticizer. Figure 7 shows number of cycles to break ( $N$ ) under the maximum constant strain. All the curves decrease monotonously with the increase of the strain. Sample A has better cut growth resistance than samples C and B.

Under constant strain, however, the stress initially given to the sample may relax during fatigue. This brings an unfairly better result on the sample with large stress relaxation. Therefore, the fatigue test should be carried out under constant stress in order to make the discussion on the cut growth resistance clear. Thus, Figure 8 shows number of cycles to break under constant stress by means

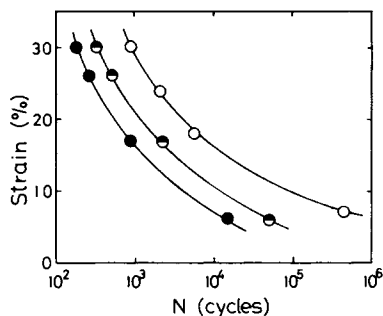


Fig. 7. Strain dependence of number of cycles to break ( $N$ ) under constant strain. (O, ●, ⊖) Samples A, B, and C, respectively.

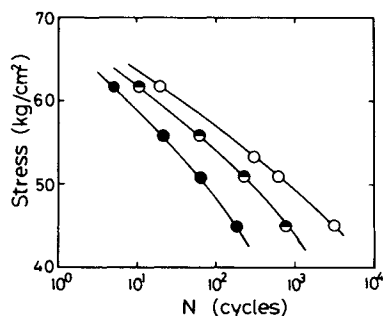


Fig. 8. Stress dependence of number of cycles to break ( $N$ ) under constant stress. (O, ●, ⊖) Samples A, B, and C, respectively.

of an Instron Universal Tester plotted against the stress. Sample A shows again the best cut growth resistance, followed by samples C and B.

Figure 9 shows the load dependence of creep ratios ( $\Delta\epsilon$ ) at 100°C. The large  $\Delta\epsilon$  for sample C seems to indicate that it owes its good cut growth resistance under the constant strain (Fig. 7) partly to the stress relaxation. On the other hand, the small  $\Delta\epsilon$  for sample A, coupled with the results from Figure 8, seems to show less stress relaxation effect.

### Stress-Strain Curves after Fatigue Tests

In order to see the changes of several mechanical properties after the tests, samples A, B, and C were fatigued in the following way. The maximum constant load of 60 kg/cm<sup>2</sup> was applied repeatedly to each sample (150 × 10 × 1 mm) without cut by means of an Instron Universal Tester. The length between the two clamps were 80 mm. The number of repetition was 8000. The other test conditions were the same as described in the Experimental section.

Stress-strain curves for the fatigued samples are shown in Figure 10. For comparison the curves for virgin samples are illustrated in the same figure. The most marked change is observed in Figure 10(b). After the fatigue the modulus at lower strain declines. At higher strain, however, the curve increases steeply, and consequently  $T_B$  reaches as high as 840 kg/cm<sup>2</sup>. On the other hand,  $E_B$  is decreased substantially. These results, except the decrease of the modulus at lower strain, imply the occurrence of some change from rubberlike structure to

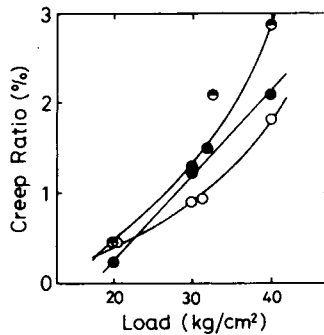


Fig. 9. Relationship between creep ratios and load at 100°C. (○, ●, ◐) Samples A, B, and C, respectively.

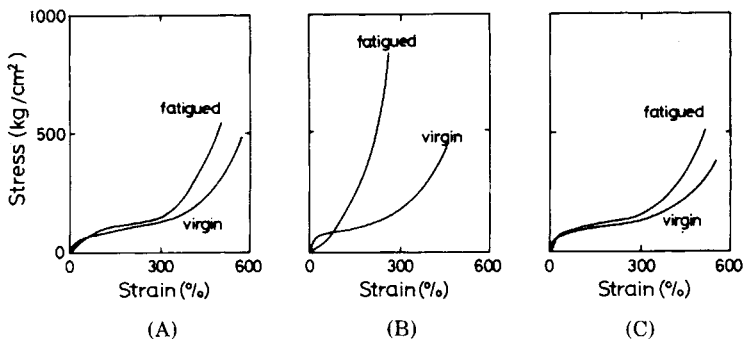


Fig. 10. Stress-strain curves for virgin and fatigued samples A, B, and C.



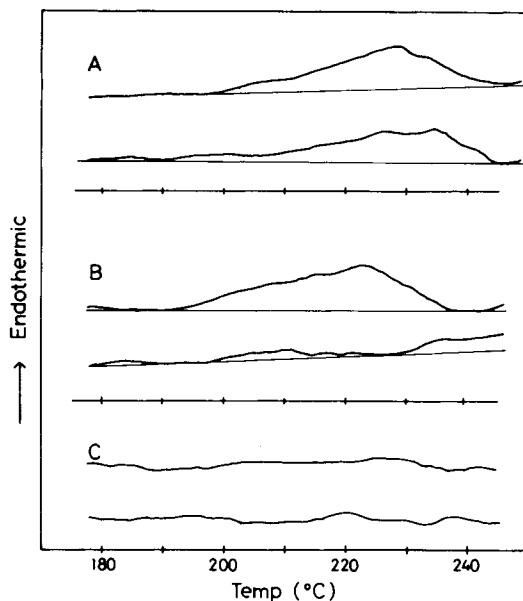


Fig. 11. DSC thermograms for virgin and fatigued samples A, B, and C. Upper: virgin; lower: fatigued; amount of each sample: 25 mg; scan rate: 5°C/min.

fiberlike one in sample B, probably because of stress-induced orientation of both hard and soft segments during the test. On the other hand, samples A and C show much less change as shown in Figures 10(a) and 10(c).

Another evidence for the orientation in the fatigued sample B is obtained from swelling tests in chloroform. The linear swelling ratios were determined in the directions parallel ( $Q_{\parallel}$ ) or perpendicular ( $Q_{\perp}$ ) to the tensile direction in the fatigue tests. The ratios of  $Q_{\parallel}/Q_{\perp}$  are given in Table IV. It is apparent from Table IV that the fatigued sample B swells to the parallel direction much less than the fatigued samples A and C. The anisotropic swelling agrees with the results from the stress-strain curves in Figure 10(b).

### Thermal Analysis after Fatigue Tests

Hard segments having a structure suitable for good molecular order are known to partly crystallize to show high melting point. Cooper reported<sup>11</sup> that polyester-based polyurethane involving 4,4'-diphenylmethane diisocyanate and

TABLE III  
Mechanical Properties for DHDM, MDDM, and DOP-Added Polyurethane Having Similar Moduli<sup>a</sup>

Sample	NCO content (wt %)	NH <sub>2</sub> /NCO	$M_{10}$ (kg/cm <sup>2</sup> )	$T_B$ (kg/cm <sup>2</sup> )	$E_B$ (%)	$\Gamma$ (kg/cm)
A <sup>b</sup>	4.99	1.00	39.0	494	580	54
B <sup>b</sup>	5.10	1.00	41.0	440	450	42
C	6.10	1.07	42.0	383	550	38

<sup>a</sup> The amount of dioctylphthalate (DOP) is 20 parts per 100 parts by weight of the prepolymer.

<sup>b</sup> Samples A and B are D-6 and M-8 in Table II, respectively.

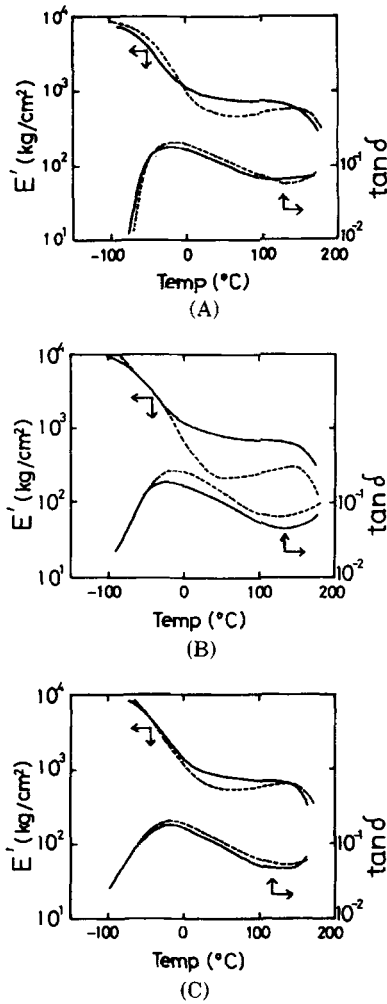


Fig. 12. Temperature dependence of storage moduli and loss tangent before and after fatigue tests: (—) virgin; (---) fatigued.

TABLE IV  
Anisotropic Swelling of Fatigued Samples A, B, and C with Chloroform

Sample	A	B	C
$Q_{\parallel}/Q_{\perp}$ <sup>a</sup>	0.85	0.61	0.86

<sup>a</sup>  $Q_{\parallel}$  and  $Q_{\perp}$  are swelling ratios parallel and perpendicular to the tensile direction of fatigue tests, respectively.

1,4-butanediol showed a peak between 200 and 220°C corresponding to the fusion of hard segments on a DSC thermogram. It is also briefly reviewed by Smith<sup>12</sup> that spherulites of hard segments are observed by x ray in Adiprene L-100 with TDI and MOCA as hard segments, as employed in this report.

Figure 11 shows the DSC thermograms for the virgin and the fatigued samples A, B, and C. The endothermic peak from 200 to 240°C observed in the virgin

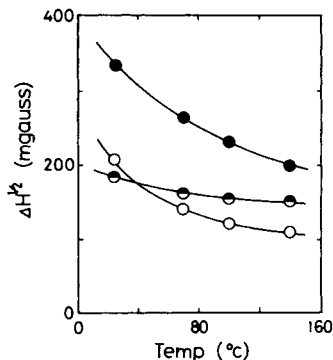


Fig. 13. Temperature dependence of NMR half-width for virgin samples A, B, and C. (○, ●, ⊙) Samples A, B, and C, respectively.

samples A and B thus appears to show the fusion of crystalline hard segments. On the other hand no clear peak is observed in the virgin sample C, probably because of the interference with the ordering by free amino groups of excessive MOCA and the plasticizer. Furthermore, it is found from Figure 11 that during the fatigue test the heat of fusion for the sample B is greatly diminished, while for sample A it is only slightly decreased. This also supports the speculation that the fatigue test damages the ordered structure of sample B to change it into the amorphous fibrous structure.

### Viscoelastic Properties after Fatigue Tests

Figure 12 shows the temperature dependence of dynamic moduli ( $E'$ ) and loss tangents ( $\tan \delta$ ) for the virgin and the fatigued samples A, B, and C. The most marked change can be seen again in the sample B. The level of  $E'$  is decreased substantially and increased with increasing temperature.  $\tan \delta$  is increased at all temperatures. The changes in samples A and C are much smaller than in sample B.

### Broad Line NMR Measurements

The molecular mobility of soft segments is one of the parameters related to the flex crack and cut growth resistance, since it dissipates energy given at a tip of a cut. At similar values of moduli, a test sample with greater molecular mobility will be expected to show better fatigue resistance because of the rapid stress relaxation at the tip of the cut. A measure of such molecular mobility can be obtained from a half-width ( $\Delta H_{1/2}$ ) of a broad line NMR.

The half-width for samples A, B, and C are plotted against temperature in Figure 13. The half-width for sample B is apparently much larger than  $\Delta H_{1/2}$  for samples A and C. Sample B is the least active in molecular motion among them. The good activity in molecular motion for sample C is caused by the added DOP, while that for sample A is ascribed to the higher molecular weight component of the PTMG mixture. The inferior cut growth resistance of sample B and the superior cut growth resistance of samples A and C may be explained in this way.

This, however, cannot explain the superiority of sample A over sample C, because sample C is more active in molecular motion than sample A at room temperature. The following hypothesis may be proposed, though we do not have enough evidence to prove at present: The stress-induced crystallization,<sup>5</sup> which stops the cut growth, will take place much easier in sample A than in sample C, since sample A has a large enough molecular weight for soft segments for their crystallization.

The authors are grateful to Tetsuya Takamatsu, director of the R. & D. Division of Bridgestone Tire Co. Ltd., for his permission for this publication. We are also grateful to Professor Junji Furukawa, Science University of Tokyo, and Dr. Shiro Anzai and Dr. Toshio Nishi, Bridgestone Tire Co. Ltd., for their valuable comments and discussion.

### References

1. E. I. du Pont de Nemours Bulletin on Adiprene Rubber (May, 1962).
2. G. S. Schollenberger and K. Dinbergs, *Adv. Urethane Sci. Technol.*, **3**, 36 (1974).
3. D. R. McGillvary, The Firestone Tire & Rubber Company, U.S. Pat. 3,701,374, October, 1972.
4. J. M. Buist and H. Gudgeon, *Advances in Polyurethane Technology*, Wiley, New York, 1968.
5. L. Morbitzer and H. Hespel, *J. Appl. Polym. Sci.*, **16**, 2697 (1972).
6. J. M. Buist, *Developments in Polyurethanes* Vol. 1, Applied Science, London, 1978, p. 53.
7. S. C. Kim, D. Klemperer, K. C. Frisch, and H. L. Frisch, *J. Appl. Polym. Sci.*, **21**, 1289 (1977).
8. K. Agei and K. Ninomiya, *Nippon Gomu Kyokaishi*, **41**, 116 (1968).
9. T. Nishi and T. Naito, Presented at the 45th Meeting of the Society of Rubber Industry, Japan, 1978.
10. K. Tsukamoto and J. Harada, The Bridgestone Tire Co. Ltd., private communication.
11. R. W. Seymour and S. L. Cooper, *J. Polym. Sci. Polym. Lett. Ed.*, **9**, 689 (1971).
12. T. L. Smith, *Rubber Chem. Technol.*, **51**, 225 (1978).

Received December 5, 1979

Accepted February 20, 1980